Model-Free Nonsingular Fast Terminal Sliding Mode Control of a Permanent Magnet Synchronous Motor

Ashraf Abdalla Hagras[1], Ayman Azab[1] and Sherif Zaid[2]

Egyptian Atomic Energy Authority (EAEA), Abo Zaabal, 13759 Cairo, Egypt; ashraf.hagras@eaea.org.eg, ayman.eisa@eaea.org.eg

Faculty of Engineering, Tabuk University, 71491 Tabuk, KSA; Shfaraj@ut.edu.sa.com

Abstract: This paper proposes a new algorithm for Model-Free Control (MFC) combined with an improved Nonsingular Fast Terminal Sliding Mode Control (NFTSMC) technique for current control of a Permanent Magnet Synchronous Motor (PMSM). This new improved NFTSMC technique adds more advantages to the conventional terminal sliding mode control theory to enhance transient and steady state performance. The proposed new improved NFTSMC bridged over the traditional difficulties of Terminal Sliding Mode Control (TSMC) theory, like the limited values of its constraints and its state differentiation and avoids the complexity of its following versions. The MFC was based on the Radial Basis Function Neural Network (RBF NN) which doesn't require known bounds of uncertainty. The stability of the proposed method was analyzed using Lypunov stability theory. Therefore, this technique was compared with Model Free Fractional Order Sliding Mode Control (MFFOSMC) [11] using MATLAB/SIMULINK in a vector control scheme to validate its design and show its faster torque and speed response, as well as its strong robust performance against varying parameters and external load disturbances.

Keywords: Model Free Control (MFC); Nonsingular Fast Terminal Sliding Mode Control (NFTSMC); Permanent Magnet Synchronous Motor (PMSM); Fractional Order Sliding Mode Control (FOSMC)

1 Introduction

PMSM played a great role in adjustable speed drives and Electric Vehicles (EVs) thanks to great features and characteristics like high power density, high efficiency, and lower maintenance. These applications exposed it to varying temperatures that affected its parameters, abrupt changes in applied loads according to the process requirements, and sharply changing speed requirements or all these conditions simultaneously.

Model-Free Control (MFC) is an effective control approach that doesn't need the process model or its parameters. Therefore, it can compensate for large parameter uncertainties and conquer high model nonlinearities using an accurate model estimator like RBF NN. RBF NN has high control accuracy, a simple structure, and fast convergence scheme to model highly nonlinear processes [1-3]. Therefore, it was motivated to be combined with other advanced nonlinear controllers [4-8]. In the early last decade, MFC was combined with Intelligent Proportional (*iP*), Intelligent Proportional Integral (*iPi*) [6] and Intelligent Proportional Differentiator (*iPD*) Controllers. But in the early part of this decade, the MFC approach was combined with advanced linear predictive controllers [9] and nonlinear controllers like fractional order sliding mode controllers [10] to add their excellent features.

Sliding mode control proved its robustness against parameter uncertainties and external disturbances, and it is simple, implantable, and easily accommodated by nonlinear controllers [11]. But it suffered from two conventional difficulties; chattering phenomena and the singularity of the solution. Second Order SMC (SOSMC) based on Super Twisting Algorithm (STA-SOSMC) gives a continuous control input proposed to eliminate chattering [12]. But it faced difficulties like gain tuning because of the system nonlinearity, and it occupied a major research field [13]. Ref. [14] overcomes this obstacle by employing rooted tree optimization to tune this gain. While Ref. [15] adapts this problem using a variable gain algorithm. But the gain and the parameters of the control law in our proposed method don't need any tuning, and its power has no restrictions compared to the conventional TSMC form.

Therefore, SMC should be enhanced to eliminate its conventional drawbacks by enhancing its sliding surface design. This motivated the creation of the Fractional Order Sliding Mode (FOSM) surface, which enhances the controller performance by adding more degrees of freedom and flexibility to support the dynamics of highly and strongly nonlinear systems and provides the role of optimizing algorithms. However, In [16], the authors not only added the exponential reaching law, but introduced Extended State Observer (ESO) design to compensate parameters changes and disturbances. In [17], designing FOSMC wasn't enough, the authors also designed a fractional order estimator to compensate for uncertainties and disturbances without prior knowledge of their bounds. In our paper, NFTSMC was in its original form without any added functions, more terms, or optimizing algorithms.

NTSMC was developed to get fast and finite convergence time, accurate tracking, and to eliminate the singularity of the solution compared to conventional TSMC. Despite that, Ref. [18] added an integral term of the conventional signum function to the integral terminal sliding mode surface to decrease the convergence time when the reference speed is far from the equilibrium point to construct the Fast Integral Terminal Sliding Mode Controller (FITSMC) to overcome the disadvantages of ITSMC. Ref. [19] designed NFTSMC based on an adaptive finite controller with adaptive tuning laws-based barrier functions to tune the adaptive controller to

strengthen the robustness of the system, speed the convergence time, and eliminate the singularity. In [20], the authors not only designed TSMC based on adaptive law but also designed the sliding mode manifold as a recursive structure of the sliding mode surface and simulated it using fuzzy control to eliminate the chattering to design Fuzzy Adaptive Terminal Sliding Mode Control (FATSMC). Ref. [21] designed a new NFTSMC surface with a new adaptive law to compensate for the unknown upper bounds of uncertainties and disturbances and increase the convergence time. But in our paper, NFTSMC wasn't supported by adaptive law, ESO, or any other controller in the whole design. Also, the reaching law is the conventional signum function to avoid any complexities in the final control input.

Therefore, the main contributions of our paper are as follows:

1) The proposed method is a new improved NFTSMC, which is a new version of TSMC that is free of the constraints of the conventional TSMC (i.e., its parameters p and q are any positive values) and doesn't need any tuning.

2) The proposed method is free of any complexities as in the previous literature, like added functions, adaptive laws, optimizing algorithms, or state differentiations.

3) A novel design of an improved NFTSMC combined with mode free control provides finite time convergence, accurate tracking, and smaller chattering than other methods in the literature.

This paper was organized as follows: The PMSM motor was modeled in Section 2. Model free, NFTSMC design and its stability analysis were presented in Section 3. RBF NN modeling was introduced in Section 4. The simulation results were given in Section 5 and conclusions were drawn in Section 6.

2 Mathematical Modeling of the PMSM

The d- and q-axis stator currents of PMSM in the rotor reference frame can be expressed as follows [10, 18]:

$$L_d \frac{di_d}{dt} = -R_s i_d + \omega_r L_q i_q + v_d \tag{1}$$

$$L_q \frac{di_q}{dt} = -R_s i_q - \omega_r L_d i_d - \omega_r \psi_f + v_q \tag{2}$$

where v_d and v_q are the stator d and q axis stator voltages respectively, R_s is the stator resistance, L_d and L_q are the d and q axis stator inductances, λ_f is the permanent magnet flux and ω_r is the electrical rotating speed and is defined as: $\omega_r = P\omega_m$, ω_m is the mechanical angular velocity of the rotor and P is the number of pole pairs.

For surface mounted PMSM, the stator d and q inductances are equal i.e., $L_d = L_q = L$. The electromagnetic torque can be expressed as:

$$T_e = \frac{3P}{2}\left(\lambda_f i_q + \left(L_d - L_q\right) i_d i_q\right) = \frac{3P}{2}\lambda_f i_q = k_t i_q \tag{3}$$

P is the number of pole pairs and k_t is the torque constant

The mechanical equation of the PMSM can expressed as follows:

$$T_e = J\frac{d\omega_m}{dt} + B\omega_m + T_L$$

J is the rotor moment of inertia, B is the viscous friction factor, and T_L represents the applied load torque disturbance.

To efficiently use the electromagnetic torque of an IPMSM, the Maximum Torque Per Ampere (MTPA) control method provides a maximum torque/current ratio, to decrease losses and increase the efficiency of the motor. In this technique, the relationship between i_d and i_q is given by [36]:

$$i^*_d = \frac{\lambda_f}{2(L_q - L_d)} - \frac{\lambda_f}{2(L_q - L_d)}\sqrt{1 + \frac{4(L_q - L_d)^2}{\lambda^2_f} i^2_q}$$

For real-time implementation of the MTPA control, the above relationship can be simplified by taking Taylor's series expansion around zero as follows:

$$i^*_d = \frac{\lambda_f}{2(L_q - L_d)} - \frac{\lambda_f}{2(L_q - L_d)}\left[\begin{array}{l} 1 + \dfrac{2(L_q - L_d)^2}{\lambda^2_f} i^2_q \\ + higher\ orders\ of\ \dfrac{4(L_q - L_d)^2}{\lambda^2_f} i^2_q \end{array}\right]$$

Neglecting the higher orders, it can be simplified to: $i^*_d = \frac{(L_d - L_q)}{\lambda_f} i^2_q$

As shown from Eq. (4), the outer loop (speed loop) can be regulated using a PI controller to get the torque reference value and the reference value of the q-axis current (i_q^*) using Eq. (3). The reference value of d-axis current (i_d^*) can be set to zero for SPMSM to obtain independent control of d and q-axis current. The d and q-axis currents can be regulated to obtain the d and q-axis stator voltages from Eq. (1) as follows:

$$v_d = L_d\frac{di_d}{dt} + R_s i_d + \omega_r L_q i_q \tag{4a}$$

$$v_q = L_q\frac{di_q}{dt} + R_s i_q + \omega_r L_d i_d + \omega_r \psi_f \tag{4b}$$

These two equations represent the current loop of the standard vector control scheme of PMSM as shown in Fig. 1.

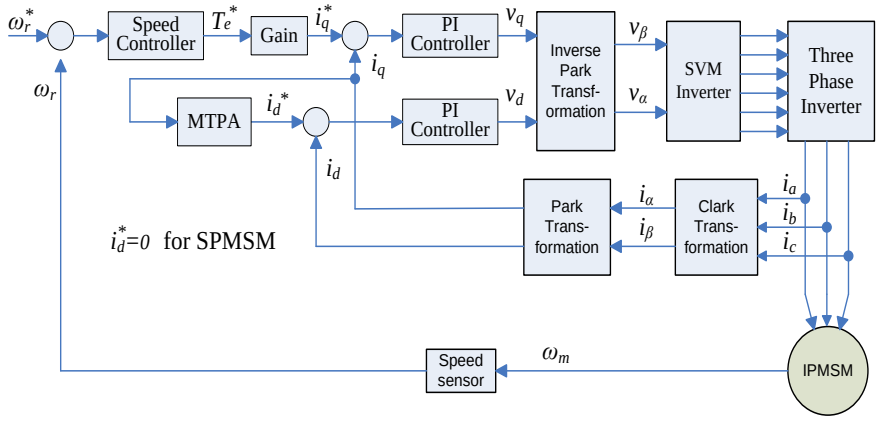

Figure 1
The block diagram of vector control scheme of PMSM

3 Model Free-NFTSMC Design and Stability Analysis

3.1 Model-Free NFTSMC Design

Model free control doesn't depend on the process or the plant model. It is local modeling of the plant from the input-output data of the plant during normal and practical conditions. MFC can be given by the following local model [4, 5, 22, 23]:

$$y^{(v)} = F(t) + \alpha * u \tag{5}$$

Where y is the control output, v is the order of differentiation of the output, u is the control input, and $F(t)$ is the estimated model obtained from the input-output data.

$$U = \frac{1}{\alpha}[y + F(t) + \gamma] = \left[y + F(t) + k_p e(t)\right]$$

Proposing the new improved NFTSM [24]:

$$S = e + \beta \int e^{(p/q)-1} \quad , p \text{ and } q \text{ any positive values, } p/q > 1 \tag{6}$$

Differentiating the new improved NFTSMC as follows:

$$\dot{S} = \dot{e} + Ke^{p/q} \tag{7}$$

The switching control input is expressed as u_s. The final model free nonsingular fast terminal sliding mode control can be expressed as:

$$u(t) = \frac{1}{\alpha}\left[k_p e(t) + k_i \int e(t) + k_d \dot{e}(t) + \dot{y}_{ref}(t) - \hat{\varepsilon}(t)\right] + u_s \tag{8}$$

Substituting Eq. (8) in Eq. (5) results in the new closed steady state error:

$$\dot{e}(t) + k_p e(t) + k_i \int e(t) + k_d e(t) + \alpha u_s + \varepsilon_m = 0 \quad (9)$$

$\hat{\varepsilon}(t)$is the estimation of the motor using RBF modeling. $\tilde{\varepsilon} = \hat{\varepsilon} - \varepsilon$, $\|\tilde{\varepsilon}\| < \varepsilon_m$

ε_m is the upper bound of the estimation error.

Therefore, the added switching control input is used to compensate for the uncertainties, external disturbances, and measurement noise. According to the sliding mode control framework, a switching function *S* is defined as the NFTSM as (6) [24].

Replacing $\dot{e}(t)$ from Eq. (8) in Eq. (7) results:

$$\dot{S} = -k_p e(t) - k_i \int e(t) - k_d \dot{e}(t) + \dot{y}_{ref}(t) - \alpha u_s - \varepsilon(t) + K e^{p/q} \quad (10)$$

To eliminate the chattering phenomena and fast finite time convergence, the following conventional fast reaching law is proposed:

$$\dot{S} = -ksign(e) \quad , k \text{ is a positive constant} \quad (11)$$

From Eq. (11) and Eq. (10), the input u_s can be defined as:

$$u_s = \frac{1}{\alpha}\left[-k_p e(t) - k_i \int e(t) - k_d \dot{e}(t) - \varepsilon_m + ksign(e) + K e^{p/q}\right] \quad (12)$$

The total input can be derived by replacing Eq. (12) with Eq. (8):

$$u = \frac{1}{\alpha}\left[\dot{y}_{ref} - \hat{\varepsilon}(t) - \varepsilon_m + ksign(e) + K e^{p/q}\right] \quad (13)$$

Applying the control Eq. (13) to the current loop of PMSM (Eq. (4)), the proposed new control equation of MFNFTSMC will be as follows:

$$v_d = \frac{1}{\alpha}\left[\dot{i_{dref}} - v_{d-neural}(t) + ksign(e) + K e^{p/q}\right] \quad (14a)$$

$$v_q = \frac{1}{\alpha}\left[\dot{i_{qref}} - v_{q-neural}(t) + ksign(e) + K e^{p/q}\right] \quad (14b)$$

The control equations of Model Free Fractional Order Sliding Mode Control (MFFOSMC) as expressed in [10]:

$$v_d = \frac{1}{\alpha}\left[\dot{i_{dref}} - v_{d-neural}(t) + kD^{\gamma} sign(e_d)^a + K sign(e_d)^b\right] \quad (15a)$$

$$v_q = \frac{1}{\alpha}\left[\dot{i_{qref}} - v_{q-neural}(t) + kD^{\gamma} sign(e)^a + K sign(e_d)^b\right] \quad (15b)$$

The structure of Model-Free NFTSMC is shown in Fig. 2.

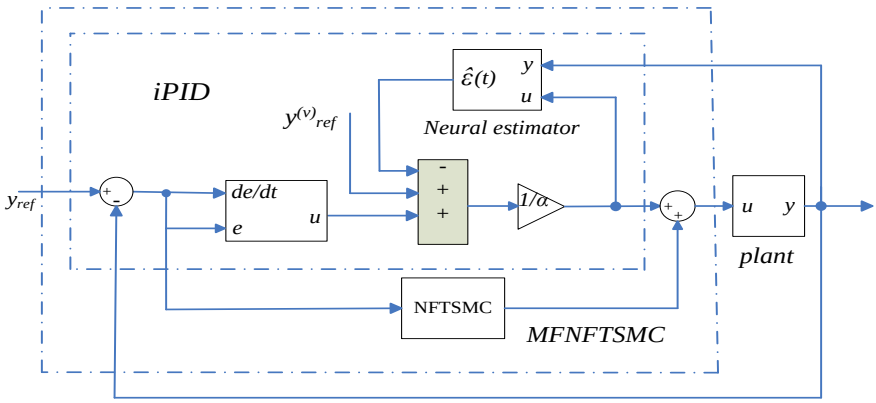

Figure 2
The structure of MF-NFTSMC

3.2 Stability Analysis

Lyapunov theory [27] has two conditions to verify the proposed sliding mode control. The first condition guarantees the system will be maintained on the sliding mode surface regardless of uncertainties and external disturbances. Therefore, the equivalent control will support that by setting the first condition, $\dot{S} = S = 0$ as obtained from Eq. (12).

The second condition should verify the reaching condition of the proposed control law, therefore, the Lyapunov candidate was chosen as follows:

$$V = (1/2)S^2$$

Differentiating the Lypunov function as follows:

$$\dot{V} = S\dot{S}$$

Substituting Eq. (13) in Eq. (5) results in:

$$\varepsilon_m - \tilde{\varepsilon} = \dot{e}(t) + ksign(e) + Ke^{p/q} \tag{16}$$

The estimated error of RBF NN modeling is defined as $\tilde{\varepsilon} = \varepsilon - \hat{\varepsilon}$

Substituting $\dot{S}$ from Eq. (7) results:

$$\dot{V} = S\left(\dot{e} + Ke^{\frac{p}{q}}\right) = -S(\tilde{\varepsilon} - \varepsilon_m + Ksign(e)) \tag{17}$$

Simplifying Eq. (17) gives the following:

$$\dot{V} = -S\big(\tilde{\varepsilon} - \varepsilon_m + Ksign(e)\big) \leq -|S[K - |\varepsilon_m - \tilde{\varepsilon}|]|$$

According to the boundedness of the error $\tilde{\varepsilon}$, $\dot{V} < 0$ if $K > 2\varepsilon_m$. Then, the right side term is negative, which ensures the stability condition of the fractional order sliding surface based on the new reaching law.

4 RBF NN Modeling and its Stability Analysis

4.1 RBF NN Modeling

Intelligent control techniques like fuzzy control and neural networks can deal with high nonlinearities due to their ability to approximate and reason about uncertain systems [25-26], and so, RBF NN is a very good model approximator. It can improve the performance of the process due to its advantages, like fast convergence and high control accuracy. The derivation of control (20) was based on the bound of the disturbance, which is known. Since the bound of the disturbance is difficult to know, we chose a large K to compensate for model uncertainties and external disturbances. At the same time, a large K leads to serious chattering. To obtain a compromise solution between attenuating the chattering and compensating the uncertainties, a RBF NN is used to estimate the plant because it has a high ability for accurate model approximation and doesn't require the known bounds of uncertainties, disturbances, or approximation errors. It is trained off-line, and the weights were obtained from MATLAB and can't be changed during the control process, which supports its real-time implementation. It has the following advantages [30-34]:

a) A partial persistency of excitation (PE) condition can be satisfied by local radial basis functions for any periodic trajectory. In this work, Gaussian radial basis functions were implemented, and they are bounded, strictly positive, absolutely integrable on compact subsets of R_n, and furthermore, they are their own Fourier transforms. Linear superposition of Gaussian RBF is the optimal solution of function approximation, given a finite set of data points in R_n.

b) Fast rate convergence, minimum training time, and better learning capability without local minima.

c) The RBF neural network reduces the computational burden with a single hidden layer and without adaptation law compared to [34-35].

The RBF network is a three-layers feedforward network. The function of the output layer is linear, where $\omega = [\omega_1, \omega_2, \ldots, \omega_n]$ and ω is the weight vector connecting the n neuron in the hidden layer and the output neuron. φ represents the activation function of each node in the hidden layer; $\varphi = [\varphi_1\ \varphi_2\ \ldots\ \varphi_n]$ and T is the output vector of the hidden layer. The Gaussian function was implemented at each node in the hidden layer. Fig. 3 displays the structure of RBF NN. Fig. 4 shows the validation, training and testing results of RBF NN modeling based on MATLAB.

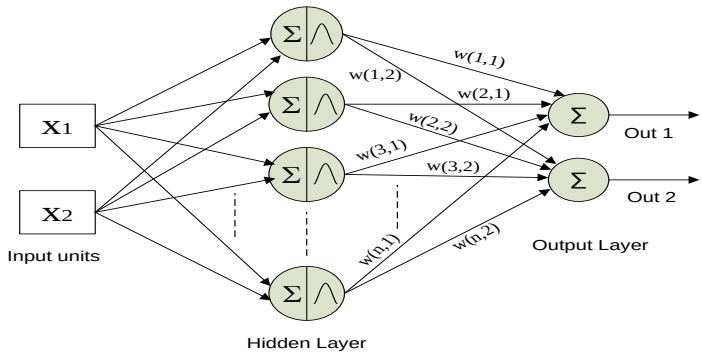

Figure 3
The structure of RBF NN

4.2 Stability Analysis of RBF NN as a Modeling Estimator

Define the tracking error as:

$$\tilde{X} = X_d - \tilde{X} \tag{18}$$

The derivative of the tracking error is:

$$\dot{\tilde{X}} = \dot{X}_d - \tilde{X} \tag{19}$$

When parameters change and external disturbances are considered, the state space equation can be reformulated as:

$$X = (A + \Delta A) + X + BU + d$$

where ΔA represents the uncertainty of A, d is the external nonlinear disturbance.

The system model can be expressed as: $X = AX + BU + F$ where F is the lumped unknown parameter uncertainties and external disturbance, expressed as $F = \Delta AX + d$.

Assumption 1: The lumped parameter uncertainties and external disturbance is bounded such that $| F | \leq F_d$, where F_d is a positive constant.

The NFTSMC sliding surface was expressed as (6): $S = e + \beta \int e^{p+q-1}$ and its derivative as (7): $\dot{S} = \dot{e} + Ke^{p/q}$.

Setting: $\dot{S} = \dot{e} + Ke^{p/q} = \dot{X}_d - AX - BU - F + Ke^{p/q}$, then the equivalent control can be expressed as:

$$U_{eq} = \frac{1}{B}\left[\dot{X}_d - AX - F + Ke^{p/q}\right] \tag{20}$$

Therefore, the sliding mode control can be expressed as:

$$U = \frac{1}{B}\left[\dot{X}_d - AX + ksign(e) + Ke^{p/q}\right] \tag{21}$$

The gain k of the switching term is an adjustable positive constant so that the switching controller can compensate for any external disturbances.

Eq. (21) can be the final sliding mode controller, but the system model A is unknown. Therefore, adaptive control should be employed to estimate the unknown system model. The estimate of system model A can be expressed as $\hat{A}$

and $\tilde{A}$ is defined as $\tilde{A} = A - \hat{A}$.

The total sliding mode control can be defined as follows:

$$U = \frac{1}{B}\left[\dot{X}_d - \hat{A}X + ksign(e) + Ke^{p/q}\right] \tag{22}$$

Choose a Lyapunov function as:

$$V = \frac{1}{2}s^T s + \frac{1}{2}tr(\tilde{A}^T \eta \tilde{A}) \tag{23}$$

Differentiating (22) with respect to time gives:

$$\dot{V}=S^T\dot{S} + \frac{1}{2}tr(\dot{\tilde{A}}^T \eta \tilde{A})=S^T(\dot{X}_d - AX - BU - F + Ke^{\frac{p}{q}})+ tr(\dot{\tilde{A}}^T \eta \tilde{A}) \tag{24}$$

Substituting the control law (22) into (24):

$$\dot{V} = S^T\dot{S} + \frac{1}{2}tr(\dot{\tilde{A}}^T \eta \tilde{A}) = S^T(\dot{X}_d - AX - BU - F + Ke^{\frac{p}{q}})+(tr(\dot{\tilde{A}}^T \eta \tilde{A})$$

$$\dot{V} = S^T\dot{S} + \frac{1}{2}tr(\dot{\tilde{A}}^T \eta \tilde{A}) = S^T(\dot{X}_d - AX - B\frac{1}{B}\left[\dot{X}_d - \hat{A}X + ksign(e) + Ke^{p/q}\right] - F + Ke^{\frac{p}{q}})+(tr(\dot{\tilde{A}}^T \eta \tilde{A})$$

Then, we can get:

$$\dot{V} = S^T((\hat{A} - A)X - \left[ksign(e) + Ke^{p/q}\right] + Ke^{\frac{p}{q}})+(tr(\dot{\tilde{A}}^T \eta \tilde{A})$$

$$\dot{V} = S^T\tilde{A}X - S^Tksign(e) + tr(\dot{\tilde{A}}^T \eta \tilde{A}) \tag{25}$$

To make $\dot{V} \dot{\leq} 0$, the adaptive laws, they are proposed as:

$$\dot{\tilde{A}}^T = \frac{XS^T}{\eta} \tag{26}$$

Where the property of the trace of the matrix is used: $tr(S^T\tilde{A}X) = tr(XS^T\tilde{A})$

Substituting (26) in (25) results: $\dot{V} = -S^Tksign(e)$

According to Assumption 1, if the gain of the switching controller is greater than the disturbance bound such that $k > F_d$: $\dot{V} \leq -|S^T|k$

Since the Lyapunov function is positive definite and the derivative of the Lyapunov function is negative definite, by Lypunov stability theory, the closed loop system of the controller (21) is asymptotically stable.

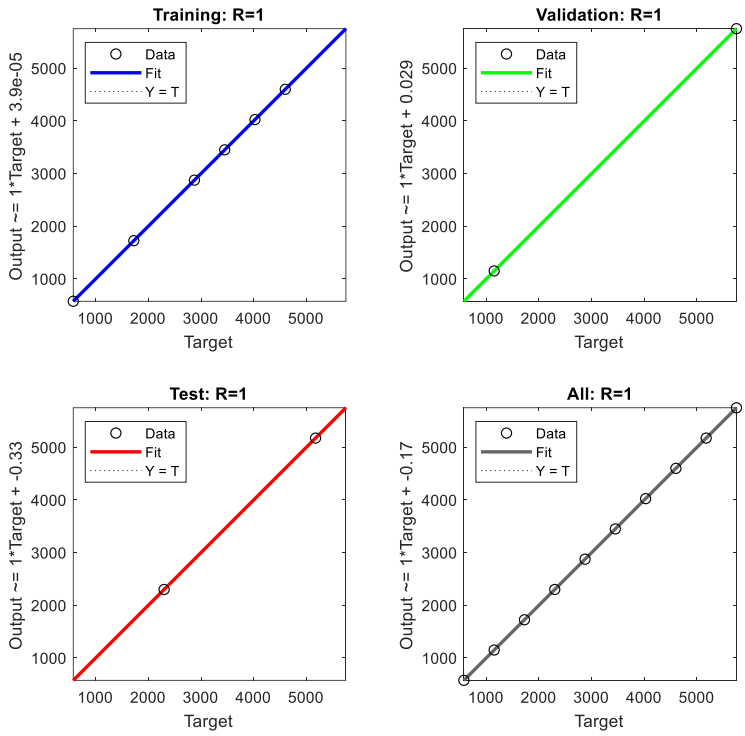

Figure 4
The validation, training, and testing results of the proposed RBF NN modeling

5 Simulation Results and Discussions

In this section, the proposed method confirms its strong robustness and superiority over other advanced sliding mode control strategies through a fair comparison with the advanced SMC method, which is Model Free Fractional Order Sliding Mode Control (MFFOSMC) [10] using (MATLAB 2018). Many tests were carried out under different operating conditions to verify its excellent transient and steady state performance and prove its strong robustness against varying parameters and external disturbances. Therefore, the comparison was carried out under the following conditions:

1) During normal conditions

2) 100% stator resistance (R_s) and inductance (L_d, L_q) uncertainties.

3) -50% stator resistance (R_s) and inductance (L_d, L_q) uncertainties.

4) Different fluxes with a higher saliency ratio of the motor

The parameters of IPMSM are as follows: R_s=2.875 ohm, L_d=L_q=12e-3 H, J=0.0008 Kg.m^2, B=0.001 N.m.s and P=4. Figs. 5 and 6 show the model of the proposed system and the proposed controller MFNFTSMC respectively.

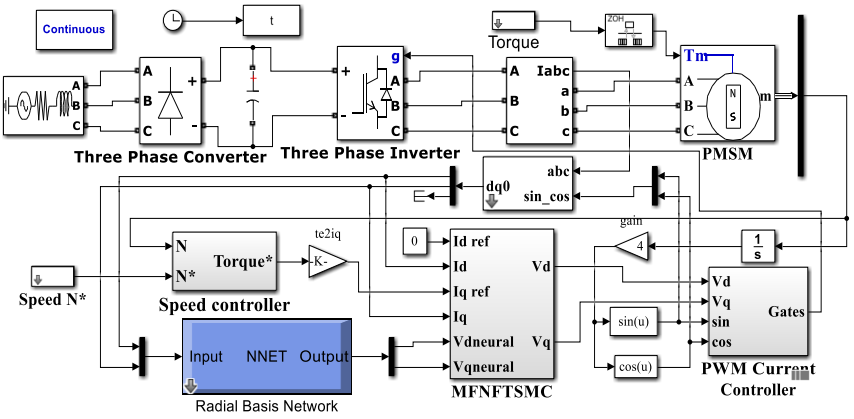

Figure 5

The MATLAB model of the proposed system

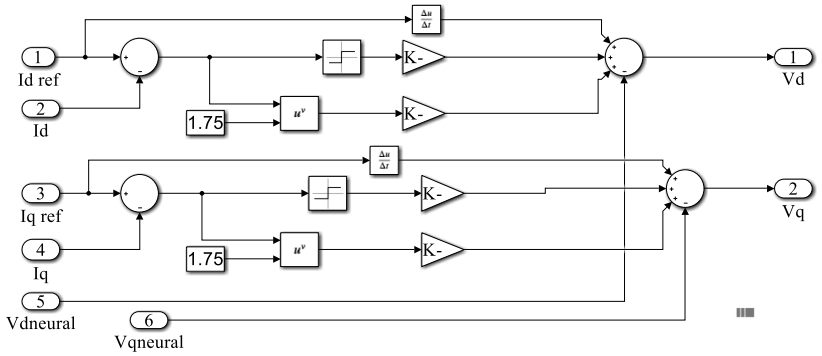

Figure 6

The MATLAB model of the proposed MFNFTSMC

5.1 During Normal Steady State Operation

In this subsection, many tests were carried out to confirm the validity, superiority of the proposed method in the transient and steady state during normal operation compared to the advanced (MFFOSMC) presented in [10].

5.1.1 Startup Response

As shown in Fig. 7, the torque startup response of the proposed method is faster than MFFOSMC. Where the rise time of the proposed method is 16.1 ms and that of MFFOSMC is 17. 1 ms. Fig. 8 displays the speed startup responses of the two

controllers. As displayed in the figure, the proposed method, MFNFTSMC, is also faster than MFFOSMC and the response of both have little overshoot. This verifies the superior torque and speed transient performance of the proposed controller compared to the advanced MFFOSMC.

5.1.2 Torque Step Change

Figure 9 depicts the step load change response of the two controllers at t=0.2 ms, where their responses may be identical in this case. Figure 10 shows that the step change in load has no effect on the speed response of the two controllers, proving the strong robustness of both controllers against external disturbances during normal operation.

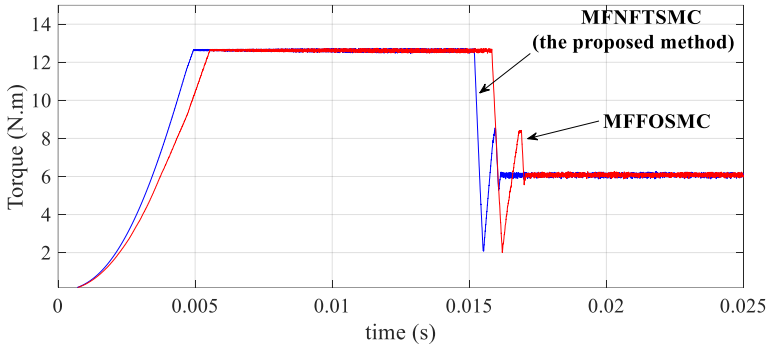

Figure 7
The torque startup response during normal conditions

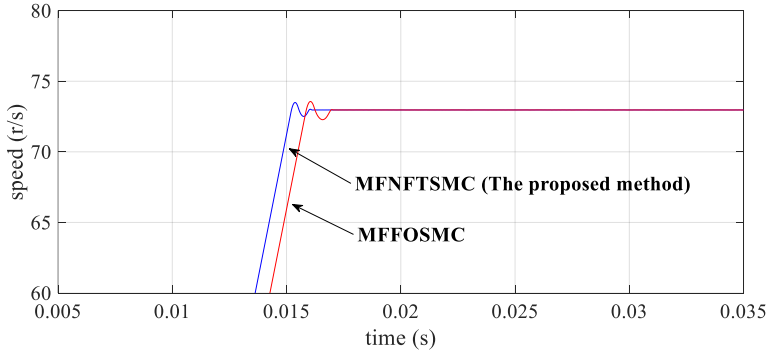

Figure 8
The speed startup response during normal conditions

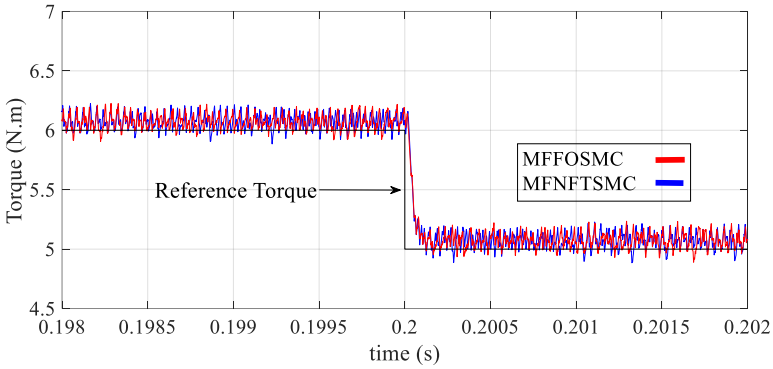

Figure 9

The step torque response during normal operation

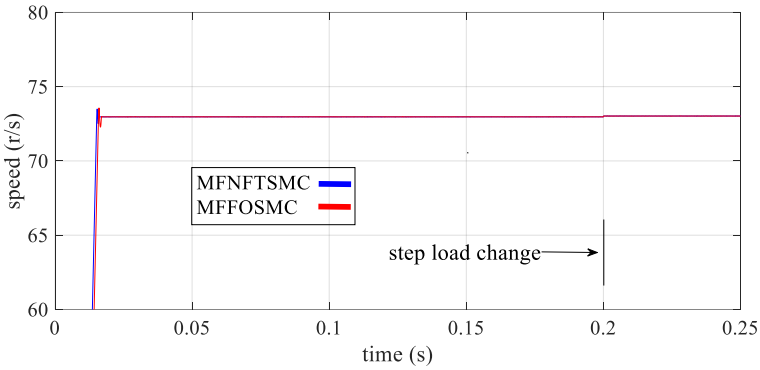

Figure 10

The speed response due to step change of load during normal operation

5.2 100% Stator Resistance (R_s) and Inductance (L_d, L_q) Uncertainties

In this test, the motor was tested for 100% uncertainties of stator resistance and inductance. The stator resistance, the *d*- and *q*- inductances values were doubled in this test.

5.2.1 Startup Response

Fig. 11 shows the torque startup response of the two controllers. As depicted in this figure, the proposed controller is still faster than MFFOSMC regardless of the 100% uncertainties of stator resistance and inductances. The response of both controllers became slower than normal operation where the rise time of the proposed controller (MFNFTSMC) is 20.5 ms and that of MFFOSMC is 23.6 ms. This confirms that

the proposed controller has stronger robustness against parameter variations than the other advanced MFFOSMC.

Fig. 12 depicts that the speed of the startup response of the proposed controller (MFNFTSMC) is faster than MFFOSMC, but the uncertainties in this test increased the speed overshoot for both controllers, which reached 1.5 rpm for the proposed controller and 3 rpm for MFFOSMC. Therefore, the proposed controller still attains its superior adaptive capability compared to the advanced MFFOSMC under 100% uncertainties.

5.2.2 Torque Step Change

Fig. 13 displays the step torque response for the two controllers from 6 N.m to 5 N.m at t= 0.2 ms. As displayed in the figure, the torque response of the proposed controller MFNFTSMC is still faster than MFFOSMC with a small value (0.1 ms). In Fig. 14, the step load change has no effect on the speed response of the controllers at t= 0.2 ms. Therefore, the two controllers still attain their excellent adaptive capability to compensate for external load step changes.

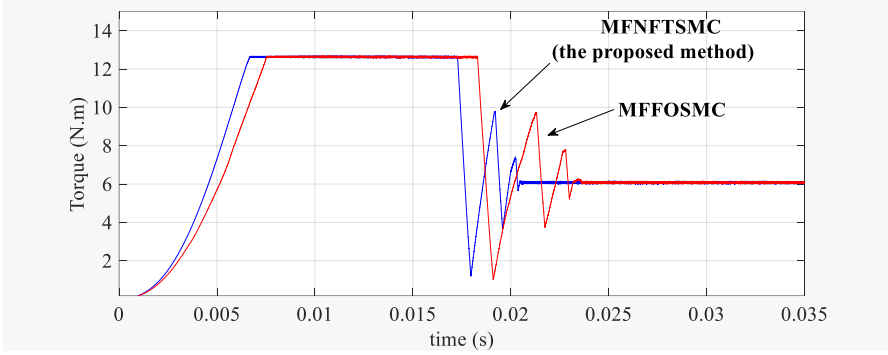

Figure 11

The torque startup response of the proposed method at 100% uncertain stator parameters

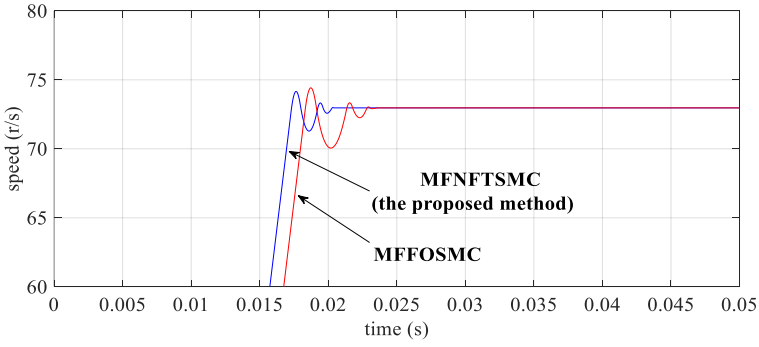

Figure 12

The speed startup response for 100% stator resistance and inductance uncertainties

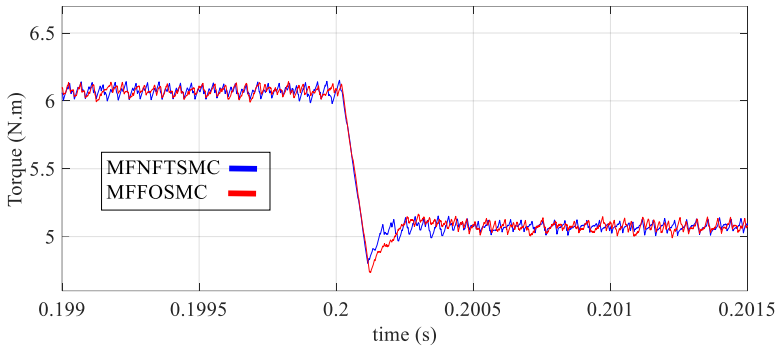

Figure 13

The torque step change response for 100% stator resistance and inductances uncertainties

5.2.3 Torque Ripples

The 100% uncertainties had a positive effect on the torque ripples, which were decreased to less than 0.2 N.m. This proves the excellent adaptive capability of both controllers, as shown in Fig. 13.

In general, in this subsection, both controllers proved they possess tremendous and superior capability under the effect of 100% uncertainties, like normal operation, with the superiority advantage of the new improved NFTSMC.

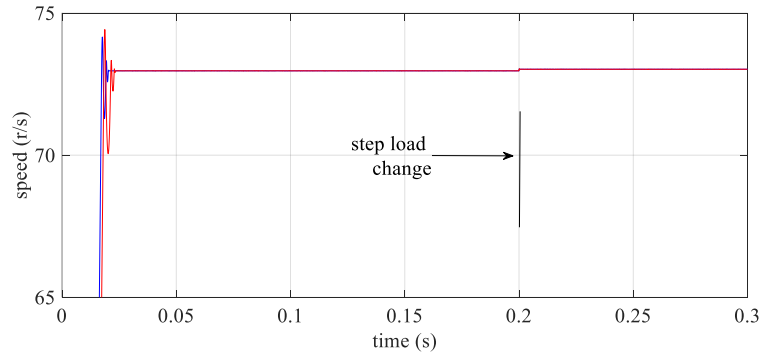

Figure 14

The speed response due to torque step change for 100% uncertainties

5.3 -50% Stator Resistance (R_s) and Inductance (L_d, L_q) Uncertainties

In this test, the motor was tested for -50% uncertainties in stator resistance and inductances. The stator resistance, the *d* and *q* inductances values were halved in this test.

5.3.1 Startup Response

Fig. 15 depicts the torque startup response of the two controllers. As depicted in Fig. 15, the proposed controller is still faster than MFFOSMC. The response became faster than normal operation, where the rise time of the proposed controller (MFNFTSMC) is 14 ms and that of MFFOSMC is 14.4 ms.

Fig. 16 depicts that the speed startup response of the proposed controller (MFNFTSMC) is faster than that of MFFOSMC, but the uncertainties in this test eliminated the speed overshoot for both controllers. Therefore, the proposed controller still attains its excellent adaptive capability compared to the advanced MFFOSMC in the transient state.

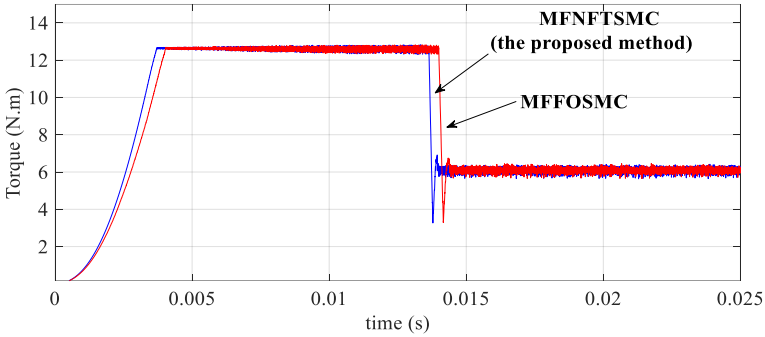

Figure 15

The torque startup response for -50% stator resistance and inductance uncertainties

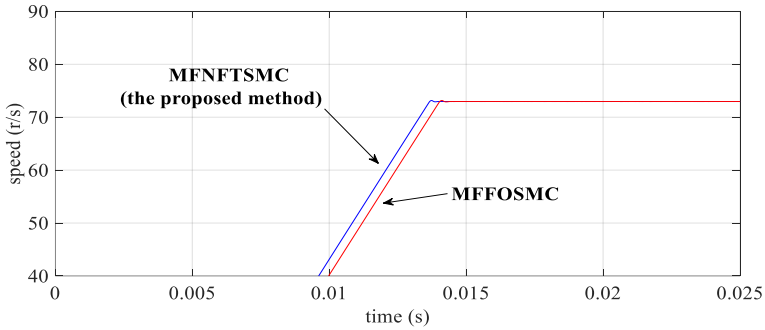

Figure 16

The speed startup response for -50% stator resistance and inductance uncertainties

5.3.2 Torque Step Change

Figure 17 depicts the step load change response of the two controllers at t=0.2 ms where their responses may be identical in this case. Figure 18 shows that the step change of load has no effect on the speed response of the two controllers, proving the strong robustness of both controllers against external disturbances under the effect of -50% stator resistance and inductance uncertainties.

5.3.3 Torque Ripples

The -50% uncertainties had a negative effect on the torque ripples when they were increased to more than 0.6 N.m. This proves the adaptive capability of the two controllers, as shown in Fig. 17. In general, in this section, the proposed controller proved it possesses tremendous and superior capability under the effect of -50% uncertainties like normal operation and 100% uncertainties.

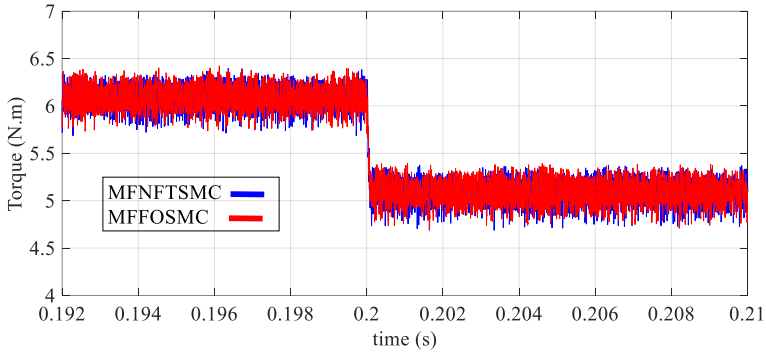

Figure 17

The torque step change response for -50% stator resistance and inductance uncertainties

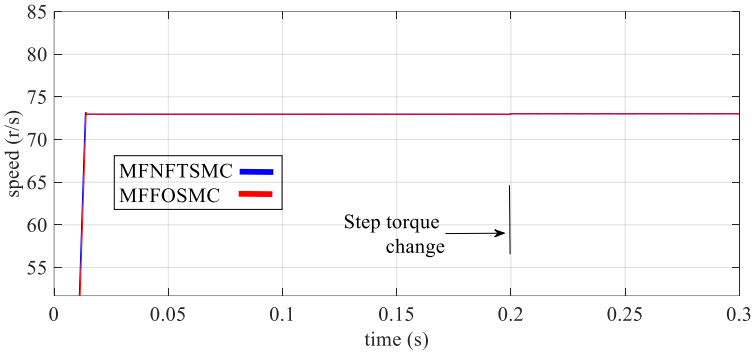

Figure 18

The speed response due to torque step change for -50% stator resistance and inductance uncertainties

5.4 Different Fluxes with a Higher Saliency Ratio of the Motor

This test verifies the excellent performance of the motor with different fluxes at higher saliencies of the motor (L_d=6 mH and L_q=12 mH). As shown in Fig. 19, the rise time increases with decreasing flux (12.3 ms, 15.3 ms and 21.2 ms). Therefore, the proposed controller attains strong and robust torque transient performance. In similar manner, the speed kept its strong robust transient performance for different fluxes, as shown in Fig. 20. Where, the rise time increases with decreasing overshoot for increasing flux and so the overshoot disappeared at flux=0.15 V.s.

Fig. 21 shows the similar minimum torque ripples for the three different values of fluxes at high saliency of the motor. The proposed controller had no effect on different fluxes and didn't affect any conditions related to its magnet flux or saliency. In this way, the proposed controller proved its optimum adaptive capability against high saliency with different fluxes for different magnets.

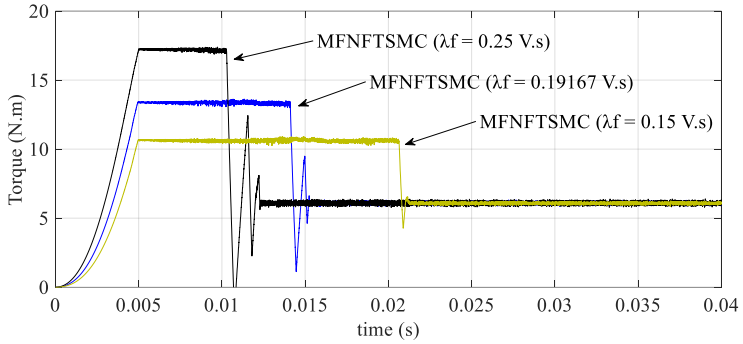

Figure 19
The torque startup for different fluxes at high saliency

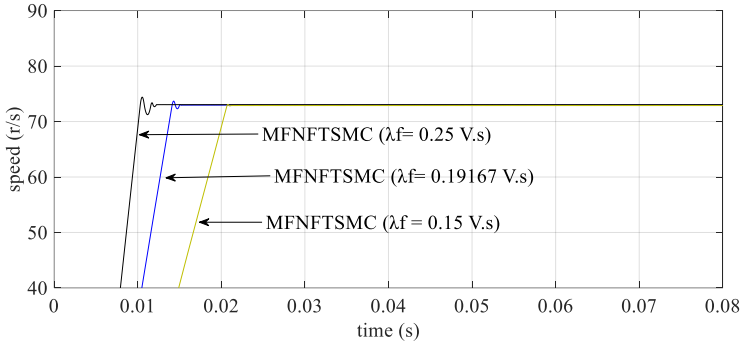

Figure 20
The speed startup for different fluxes

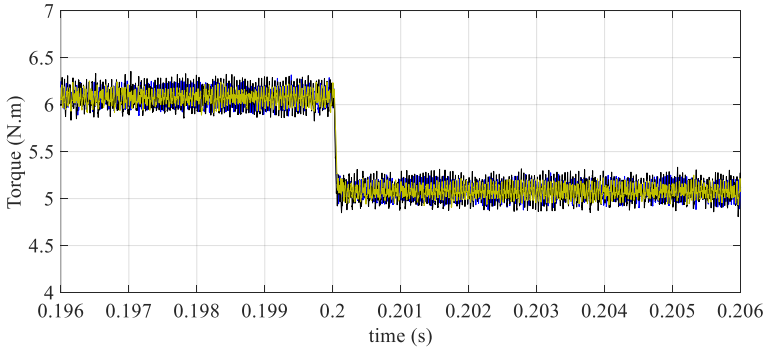

Figure 21
The torque step response for different fluxes

Conclusions

A successful design and application of a novel algorithm of Model Free Control (MFC) combined with an improved NFTSMC was proved through a fair comparison with the advanced Model Free Fractional Order Sliding Mode Controller (MFFOSMC). The proposed method proved its adaptive capability during normal operation and against long ranges of uncertainties (time varying) in electrical and mechanical parameters. A MATLAB/SIMULINK simulation validation for the proposed controller applied to PMSM. The system response with the proposed controller, MFNFTSMC, is compared to that controlled using MFFOSMC. The simulation results of the proposed method have been proved its strong robust capability against different disturbances in the load torque and commanded speed. In all scenarios of operation, the speed and torque, of the MFNFTSMC, have the faster response, lower steady state error, and the minimum speed and torque ripples. Also, it offered strong, robust transient, and steady state performance against different flux and parameter variations at high saliency of the motor. These achievements are thanks to more degrees of freedom imposed by the control terms in the new improved NFTSMC structure.

References

[1] Zhijia Zhao; Weitian He; Chaoxu Mu; Tao Zou, Keum-Shik Hong and Han-Xiong Li "Reinforcement Learning Control for a 2-DOF Helicopter With State Constraints: Theory and Experiments", IEEE Transactions on Automation Science and Engineering, Vol. 21, No. 1, 2024, pp. 157-167

[2] Jiawei Ma; Huanqing Wang and Junfei Qiao," Adaptive Neural Fixed-Time Tracking Control for High-Order Nonlinear Systems", IEEE Transactions on Neural Networks and Learning Systems, Vol. 35, No. 1, 2024, pp. 707-717

[3] Junfei Qiao; Dapeng Li; Honggui Han, "Neural Network-Based Adaptive Tracking Control for Denitrification and Aeration Processes With Time Delays", IEEE Transactions on Neural Networks and Learning Systems, 2023 (Early Access)

[4] Radu-Emil Precup, Raul-Cristian Roman, and Ali Safaei" Data Driven Model-Free Controllers", CRC Press, Taylor & Francis Group, LLC, 2022

[5] R.-E. Precup, R.-C. Roman, E.-L. Hedrea, E. M. Petriu, C.-A. Bojan-Dragos," Data-Driven Model-Free Sliding Mode and Fuzzy Control with Experimental Validation", International Journal of computers Communications & Control, Vol. 16, No. 1, 2021, pp. 1-17

[6] S. Li, H. Wang, Y. Tian, A. Aitouch and J. Klein,"Direct power control of DFIG wind turbine systems based on an intelligent proportional-integral sliding mode control", ISA Transactions, Vol. 64, 2016, pp.431-439

[7] Radu-Emil Precup, Mircea-Bogdan Radac, Raul-Cristian Roman, Emil M. Petriu," Model-free sliding mode control of nonlinear systems: Algorithms and experiments", Information Sciences, Vol. 381, 2017, pp. 176-192

[8] Dezhi Xu, Xiaoqi Song, Wenxu Yan, Bin Jiang,"Model-free adaptive command-filtered-backstepping sliding mode control for discrete-time high-order nonlinear systems", Information Sciences, Vol. 485, 2019, pp. 141-153

[9] Ahmad Reda, Rabab Benotsmane, Ahmed Bouzid, József Vásárhelyi," A Hybrid Machine Learning-based Control Strategy for Autonomous Driving Optimization", Acta Polytechnica Hungarica, Vol. 20, No. 9, 2023, pp. 165-186

[10] Ashraf Hagras, Abdelnasser Nafeh, "Model Free Fractional Order Sliding Mode Control of Permanent Magnet Synchronous Motor", International Journal of Modeling, Identification and Control, Vol. 38, No. 2, 2021, pp. 121-134

[11] Bo Long (Phd), PengJie Lu, Danny Zhan, Xin Lu, José Rodríguez, Josep M. Guerrero, Kil to Chong," Adaptive fuzzy fractional-order sliding-mode control of LCL-interfaced grid-connected converter with reduced-order", ISA Transactions, Vol. 7, 2023, pp. 557-572

[12] Abdelkarim Ammar, Amor Bourek and Abdelhamid Benakcha," Nonlinear SVM-DTC for induction motor drive using input-output Feedback linearization and high order sliding mode control", ISA Transactions, Vol. 67, 2017, pp. 428-442

[13] Yuri Shtessel, Mohammed Taleb and Franck Plestan," A novel adaptive-gain super twisting sliding mode controller: Methodology and application", Automatica, Vol. 48, 2012 pp. 759-769

[14] A. Benamor, M. T. Benchouia, K. Srairi, M. E. H. Benbouzid,"A novel rooted tree optimization apply in the high order sliding mode control using super-twisting algorithm based on DTC scheme for DFIG", Electrical Power and Energy Systems, Vol. 108, 2019, pp. 293-302

[15] K. Liao, Y. Xu and H. Zhou,"A robust damping controller for DFIG based on variable-gain sliding mode and Kalman filter disturbance observer", Electrical Power and Energy Systems, Vol. 107, 2019, pp. 569-576

[16] Ziwei Wang, Wenliang Yin, Lin Liu, Yue Wang, Cunshan Zhang, and Xiaoming Rui,"Fractional-order Sliding Mode Control of Hybrid Drive Wind Turbine for Improving Low-voltage Ride-through Capacity", IEEE Journal of Modern Power Systems and Clean Energy, Vol. 11, No. 5, September 2023, pp. 1427-1436

[17] Sadegh Ebrahimkhani," Robust fractional order sliding mode control of doubly-fed induction Generator (DFIG)-based wind turbines", ISA Transactions, Vol. 63, 2016, pp. 343-354

[18] Tian Yang, Yongting Deng, Hongwen Li, Zheng Sun, Haiyang Cao, Zongen Wei," Fast integral terminal sliding mode control with a novel disturbance observer based on iterative learning for speed control of PMSM", ISA Transactions, Vol. 134, 2023, pp. 460-471

[19] Saleh Mobayen, Farhad Bayat, Sami ud Din, Mai The Vu," Barrier function-based adaptive nonsingular terminal sliding mode control technique for a class of disturbed nonlinear systems", ISA Transactions, Vol. 134, 2023, pp. 481-496

[20] Zhe Sun, Shujie Hu, Hao Xie, Hongyu Li, Jinchuan Zheng, Bo Chen," Fuzzy adaptive recursive terminal sliding mode control for an agricultural omnidirectional mobile robot", Computers and Electrical Engineering, Vol. 105, 2023, pp. 108529-108546

[21] Saleh Mobayen, Fayez F. M. El-Sousy, Khalid A Alattas, Omid Mofid, Afef Fekih, Thaned Rojsiraphisal," Adaptive fast-reaching nonsingular terminal sliding mode tracking control for quadrotor UAVs subject to model uncertainties and external disturbances", Ain Shams Engineering Journal, Vol. 14, 2023, pp. 102059-102063

[22] Wang H. P., Ghazally I. Y. Mustafa, Y. Tian, "Model-free fractional-order sliding mode control for an active vehicle suspension system", Advances in Engineering Software, Vol. 115, 2018, pp. 452-462

[23] Michel FLIESS, Cédric JOIN, "Model-Free Control and Intelligent PID Controllers: Towards a Possible Trivializations of Nonlinear Control", Proceedings of the 15th IFAC Symposium on System Identification, Saint-Malo, France, July 6-8, 2009

[24] Ashraf Hagras, Ahmed Alaa Mahfouz," Speed Control of Single Phase Induction Motor Using New Improved Nonsingular Fast Terminal Sliding Mode Control", 2022 23rd IEEE International Middle East Power Systems Conference (MEPCON 2022), Cairo, Egypt, 13-15 Dec., 2022

[25] Radu-Emil Precup, Stefan Preitl, Emil M. Petriu, Claudia-Adina Bojan-Dragos, Alexandra-Iulia Szedlak-Stinean, Raul-Cristian Roman, Elena-Lorena Hedrea," Model-based fuzzy control results for networked control systems", Reports in Mechanical Engineering, Vol. 1, No. 1, 2020, pp. 10-25

[26] Radu-Emil Precup; Stefan Preitl, József K. Tar, Marius L. Tomescu, Márta Takacs, Péter Korondi, Péter Baranyi," Fuzzy control system performance enhancement by iterative learning control", IEEE Transactions on Industrial Engineering, Vol. 55, No. 9, 2008, pp. 3461-3475

[27] Marius-Lucian Tomescu, Stefan Preitl, Radu-Emil Precup and József K. Tar," Stability Analysis Method for Fuzzy Control Systems Dedicated Controlling Nonlinear Processes", Acta Polytechnica Hungarica, Vol. 4, No. 3, 2007, pp. 127-141

[28] Raul-Cristian Roman, Radu-Emil Precup, Elena-Lorena Hedrea, Stefan Preitl, Iuliu Alexandru Zamfirache, Claudia-Adina Bojan-Dragos, Emil M Petri," Iterative Feedback Tuning Algorithm for Tower Crane Systems," Procedia Computer Science 199, 2022, pp. 157-165

[29] Maria-Geanina UNGURITU and Teodor-Constantin NICHITELEA," Design and Assessment of an Anti-lock Braking System Controller", Romanian Journal of Information Science and Technology, Vol. 26, No. 1, 2023, pp. 21-32

[30] Ashraf Hagras," Neural Network based Direct Adaptive Control of Permanent Magnet Synchronous Motor", Journal of Electrical Engineering, Vol. 17, No. 4, 2017, pp. 322-329

[31] Jozef Ban, Matej Féder, Miloš Oravec, Jarmila Pavlovičová," Non-Conventional Approaches to Feature Extraction for Face Recognition", Acta Polytechnica Hungarica, Vol. 8, No. 4, 2011, pp. 75-90

[32] Lionel Leroy Sonfack1, Godpromesse Kenné and Andrew Muluh Fombu, "An improved adaptive RBF neuro-sliding mode control strategy: Application to a static synchronous series compensator controlled system", International Transactions on Electrical Energy Systems, Vol. 29, No. 5, May 2019

[33] Jinpeng Yu, Peng Shi, Wenjie Dong, Bing Chen and Chong Lin," Neural Network-Based Adaptive Dynamic Surface Control for Permanent Magnet Synchronous Motors", IEEE Transactions on Neural Networks and Learning Systems, Vol. 26, No. 3, pp. 640-645, 2015

[34] Yundi Chu, Juntao Fei and Shixi Hou, "Adaptive Global Sliding-Mode Control for Dynamic Systems Using Double Hidden Layer Recurrent Neural Network Structure", IEEE Transactions on Neural Networks and Learning Systems, Vol. 31, No. 4, 2020, pp. 1297-1309

[35] Juntao Fei and Huan Wang," Experimental Investigation of Recurrent Neural Network Fractional-order Sliding Mode Control of Active Power Filter", IEEE Transactions on Circuits and Systems II: Express Briefs, Vol. 67, No. 11, 2020, pp. 2522-2526

[36] Gilbert Foo and M. F. Rahman, "Sensorless Sliding-Mode MTPA Control of an IPM Synchronous Motor Drive Using a Sliding-Mode Observer and HF Signal Injection" IEEE Transactions on Industrial Electronics, Vol. 57, No. 4, April 2010